Nuclear Engineering and Technology 54 (2022) 1195–1205

Contents lists available at ScienceDirect

Nuclear Engineering and Technology

journal homepage: www.elsevier.com/locate/net

Original Article

On the use of spectral algorithms for the prediction of short-lived volatile fission product release: Methodology for bounding numerical error

G. Zullo, D. Pizzocri, L. Luzzi*

Politecnico di Milano, Department of Energy, Nuclear Engineering Division, Via La Masa 34, 20156, Milan, Italy

ARTICLE INFO

Article history:
Received 7 May 2021
Received in revised form
17 October 2021
Accepted 19 October 2021
Available online 28 October 2021

Keywords:
Fission product release
Spectral diffusion algorithms
Diffusion-decay equation
Error analysis

ABSTRACT

Recent developments on spectral diffusion algorithms, i.e., algorithms which exploit the projection of the solution on the eigenfunctions of the Laplacian operator, demonstrated their effective applicability in fast transient conditions. Nevertheless, the numerical error introduced by these algorithms, together with the uncertainties associated with model parameters, may impact the reliability of the predictions on short-lived volatile fission product release from nuclear fuel. In this work, we provide an upper bound on the numerical error introduced by the presented spectral diffusion algorithm, in both constant and time-varying conditions, depending on the number of modes and on the time discretization. The definition of this upper bound allows introducing a methodology to *a priori* bound the numerical error on short-lived volatile fission product retention.

1. Introduction

Short-lived volatile fission products greatly contribute to the equivalent dose potentially connected to nuclear accidental scenarios. As a consequence, fission product release predictions must consider the natural radioactive decay of these isotopes [1]. Predicting the release of radioactive volatile fission products from nuclear fuel is crucial in assessing radiological consequences of design-basis accidents, especially when dealing with short-lived fission products and evaluating the so-called source term for reactor safety analysis and licensing procedures [2,3]. The first step in modelling the release of radioactive volatile fission products requires the solution of a diffusion-decay partial differential equation on the scale of fuel grain [1,4]. Several fuel performance codes tackle the intra-granular gas behaviour problem through spectral diffusion algorithms (e.g., TRANSURANUS [5], BISON [6]). The development and verification of the PolyPole algorithm [7,8] demonstrated the effectiveness of spectral diffusion algorithms applied to the simulation of fission gas behaviour during fast transients in the frame of BISON code development [9].

The error introduced by the numerical discretization of the governing diffusion-decay equation, in general, must not overcome the uncertainties associated with model parameters. In nuclear safety analysis numerical error may impact the reliability of the predictions on radioactive volatile fission product release from nuclear fuel with the risk of jeopardising the licensing procedure. This work investigates the error introduced by the spectral diffusion algorithm adopted in the grain-scale code SCIANTIX [10] to compute both stable fission gas and radioactive volatile fission product release, as for the work of Hermansson and Massih [11] who investigated the accuracy of the FORMAS spectral diffusion algorithm considering only stable fission gas release [12,13]. The goal of this work is hence to propose a methodology to select the proper *a priori* condition to apply the presented spectral diffusion algorithm, being able to limit the numerical error.

In Section 2, we apply the spectrum-temporal discretization to the non-dimensional diffusion-decay equation. The non-dimensional description allows considering stable or radioactive fission products, different model parameters (e.g., the diffusion coefficient and the grain radius) and different operative conditions (e.g., temperature and fission rate) with a single analysis. The numerical solution is computed, and a quasi-analytical solution is provided as reference for the error analysis. In Section 3, we define an upper bound on the numerical error and we develop the error analysis for stable and radioactive fission products, during constant and time-varying conditions. In Section 4, we provide a

* Corresponding author.
E-mail address: lelio.luzzi@polimi.it (L. Luzzi).

https://doi.org/10.1016/j.net.2021.10.028

Nomenclature

D	(m^2 s^{-1}) Single gas atom intra-granular diffusivity
λ	(s^{-1}) Decay rate of the fission product
S	(at $m^{-3}s^{-1}$) Production rate of the fission product
y	(at $fiss^{-1}$) Fission product yield
ρ	(/) Non-dimensional radial coordinate in the spherical grain
τ	(/) Non-dimensional temporal coordinate
ϕ	(/) Non-dimensional intra-granular fission product concentration
a	(m) Radius of the ideal spherical fuel grain
T	(K) Fuel temperature
F	(fiss m^{-3} s^{-1}) Fission rate density
ψ_n	(/) n-th normalized eigenfunction of the spherical Laplace operator
θ_n	(/) n-th eigenvalue of the spherical Laplace operator
x_n	(/) n-th temporal coefficient
δ_{nj}	(/) Kronecker delta
μ	(/) Non-dimensional group of the diffusion-decay equation
$\overline{\phi}$	(/) Spatial average of the non-dimensional intra-granular fission product concentration
$\overline{\phi}_A$	(/) Quasi-analytical solution for the spatial average of the non-dimensional concentration
$\overline{\phi}_N$	(/) Numerical solution for the spatial average of the non-dimensional concentration
err	(/) Numerical error between the numerical and the quasi-analytic solution for the spatial average of the concentration
ε	(/) Upper bound on the numerical error between the numerical and the quasi-analytic solution for the spatial average of the concentration
$\varepsilon_{\Delta\tau}$	(/) Temporal contribution to the upper bound on the numerical error
ε_M	(/) Modal contribution to the upper bound on the numerical error
$\widehat{\varepsilon}$	(/) Polynomial fit of the upper bound on the numerical error

methodology for the *a priori* choice of the time step and mode number to be used in the presented spectral diffusion algorithm, according to a demanded upper bound on the numerical error. Lastly, Appendices A, B and C showcase the application and verification of the proposed methodology in selecting the time step and mode number, according to a demanded upper bound on the numerical error.

2. Spectral algorithm

Diffusion-decay models allow for the description of intra-granular behaviour of volatile fission products in nuclear oxide fuel [1,14–18]. These models describe the fission product diffusion in a spherical homogenous fuel grain, of radius a (m), at uniform temperature T (K) and experiencing a uniform fission rate density F (fiss m^{-3} s^{-1}). We consider the following partial differential equation:

$$\frac{\partial C(r,t)}{\partial t} = D(F,T)\nabla^2 C\left(r,t\right) - \lambda C\left(r,t\right) + S(F),\ r\in[0,a),\ t>0 \tag{1}$$

in which the variables depend on the time t (s) and radial position r (m). Eq. (1) is formulated with the initial condition $C(r,0)=C_0$ on $r\in[0,a)$, boundary conditions $C(a,t)=0$ and $\left(\frac{\partial C(r,t)}{\partial r}\right)_{r=0}=0$ for $t>0$. C(at m^{-3}) is the intra-granular fission product concentration, D (m^2 s^{-1}) is the diffusivity [19], λ (s^{-1}) is the decay rate, $S=yF$ (at $m^{-3}s^{-1}$) is the production rate of the fission product, being y (at $fiss^{-1}$) the fission yield. Besides, in Eq. (1) we exploit the weak variation of the diffusivity D on the radial position r in the fuel grain to assume that $-\nabla\cdot(-D(F,T)\nabla C(r,t)) = D(F,T)\nabla^2 C(r,t)$. We write the non-dimensional version of Eq. (1) by posing $\rho = r/a$, $\tau = tD/a^2$, $\phi = CD/a^2S$ and $\mu = \lambda a^2/D$ to get

$$\frac{\partial\phi(\rho,\tau)}{\partial\tau} = \tilde{\nabla}^2\phi(\rho,\tau) - \mu(\tau)\phi(\rho,\tau) + 1,\ \rho\in[0,1),\ \tau>0 \tag{2}$$

It is worth clarifying that, among possible normalizations, the proposed one is well defined when stable fission products are considered, i.e., $\lambda=0$, but requires minor modifications to account for out-of-pile conditions, as explained in Appendix B. The initial condition for Eq. (1) translates into $\phi_0 = C_0D/a^2S$ and the non-dimensional radial spherical Laplacian is noted as $\tilde{\nabla}^2$. Then we apply the following modal expansion of the concentration up to the N_M-th term

$$\phi(\rho,\tau) = \sum_{n=1}^{N_M} x_n(\tau)\psi_n(\rho) \tag{3}$$

with the chosen spatial modes $\psi_n(\rho)$ being the normalized eigenfunctions of the spherical Laplace operator, $\psi_n(\rho) = \frac{1}{\sqrt{2\pi}}\frac{\sin(\theta_n\rho)}{\rho}$, $\theta_n = n\pi$, the unknown of the problem becomes the set of time coefficients $\{x_n(t)\}$. The latter are the solution of the problem:

$$\sum_{n=1}^{N_M}\frac{\mathrm{d}x_n(\tau)}{\mathrm{d}\tau}\delta_{nj} = -\sum_{n=1}^{N_M}x_n(\tau)\left(\theta_n^2+\mu(\tau)\right)\delta_{nj} + \langle\psi_j|1\rangle \tag{4}$$

where $\langle\psi_n|\psi_j\rangle = \int_\Omega \psi_n\psi_j\mathrm{d}\Omega = \delta_{nj}$ is the Kronecker delta and $\langle\psi_j|1\rangle = \frac{(-1)^{j+1}}{j}\sqrt{\frac{8}{\pi}}$. For every time coefficient the following ordinary differential equation is hence to be solved:

$$\frac{\mathrm{d}x_j(\tau)}{\mathrm{d}\tau} = -\Lambda_j(\tau)x_j(\tau) + \langle\psi_j|1\rangle \tag{5}$$

where the mode eigenvalue is $\Lambda_j(\tau)=\theta_j^2+\mu(\tau)$ and the initial condition comes from the projection $x_j(0)=\langle\psi_j|\phi_0\rangle$.

We briefly sketch the numerical scheme adopted in SCIANTIX [10] to solve Eq. (5). The time-interval $(0,\tau_f)$ is divided in $N_{\Delta\tau}$ time-steps, and by exploiting the backward Euler scheme we compute, for each time-step:

$$x_{j,N}^{k+1} = \frac{x_{j,N}^k + \langle\psi_j|1\rangle\Delta\tau}{1+\Lambda_j^{k+1}\Delta\tau} \tag{6}$$

where the superscript k indicates the discrete time $\tau^k = k\Delta\tau$. For

every time-step, the temporal coefficients $x_{j,N}^{k+1}$ are evaluated and the spatial average of the concentration $\left(\bar{\phi} = \frac{3}{4\pi}\sum_{j=1}^{N} x_j\langle\psi_j|1\rangle\right)$ is reconstructed. When the temporal coefficients are given by Eq. (6), we mark the spatial average of the concentration $\bar{\phi}$ with the subscript N:

$$\bar{\phi}_N^{k+1} := \frac{3}{4\pi}\sum_{j=1}^{N_M}\frac{x_{j,N}^{k} + \langle\psi_j|1\rangle\Delta\tau}{1+\Lambda_j^{k+1}\Delta\tau}\langle\psi_j|1\rangle \tag{7}$$

Since the temporal coefficients $x_j(\tau)$ are computed by exploiting a numerical discretization scheme (Eq. (6)), we refer to Eq. (7) as the numerical solution (of our interest).

To carry out the next error analysis, and hence verify our numerical solution (Eq. (7)), we introduce a quasi-analytical formulation for the spatial average of the concentration $\bar{\phi}$, labelled with the subscript A, as:

$$\bar{\phi}_A^{k+1} := \frac{3}{4\pi}\sum_{j=1}^{CN_M}\left(\frac{\langle\psi_j|1\rangle}{\Lambda_j^{k+1}}\left(1-\exp\left(-\Lambda_j^{k+1}\frac{\Delta\tau}{M}\right)\right) + x_{j,A}^{k}\exp\left(-\Lambda_j^{k+1}\frac{\Delta\tau}{M}\right)\right)\langle\psi_j|1\rangle \tag{8}$$

Constant conditions are assumed within each time-step. We refer to Eq. (8) as the quasi-analytic solution, in contrast with the numerical solution (Eq. (7)). The main difference with the latter formulation lies in the temporal coefficient $x_{j,A}^{k+1}$, evaluated at each time step from the exact solution of Eq. (5), with an incremental approach. Besides, Eq. (8) is obtained by using a higher number of time-steps $N_{\Delta\tau}$ (by a factor of $M \gg 1$) and a higher number of modes N_M (by a factor of $C \gg 1$) with respect to Eq. (7), to increase its accuracy.

The presented error analysis exploits a quasi-analytic reference solution that is in line with the reference solution used as reference by Lassmann and Benk for the verification of URGAS and FORMAS [20], namely, the quasi-exact ANS-5.4 algorithm [21]. In the current fuel performance codes, the spectral diffusion algorithms represent the state-of-the-art approach to solve the intra-granular stable fission gas diffusion. To provide a straightforward application of our work, we tailored our error bound methodology on the presented spectral diffusion algorithm, extended to include the radioactive decay. Different error analysis, e.g., based on the global spectral analysis [22–24], are of interest for future developments, towards the innovation of the presented algorithm.

3. Error analysis

The goal of this section is to analyse the error introduced by the presented spectral diffusion algorithm adopting the backward Euler time discretization and to provide an upper bound on it.

We propose the following definition for the error between the numerical solution (Eq. (7)) and the quasi-analytic solution (Eq. (8)):

$$\mathrm{err}(N_{\Delta\tau}, N_M;\mu) := \max\left(\left|\frac{\bar{\phi}_A(\tau)-\bar{\phi}_N(\tau)}{\bar{\phi}_A(\tau)}\right|\right) \tag{9}$$

where $N_{\Delta\tau}$ and N_M are the number of time-steps and the number of modes used in the computation of the numerical solution (Eq. (7)). In the definition of the error, we assume that M and C, introduced in Eq. (8), are high enough to have a negligible impact on the error itself.

The diffusion-decay equation (Eq. (2)) is numerically solved on the interval, $\tau \in (0, \tau_e)$, being τ_e the time required from the concentration ϕ to reach equilibrium. In constant conditions, $\tau_e \approx \frac{5}{\pi^2+\mu}$, or $t_e \approx \frac{5}{\frac{D\pi^2}{a^2}+\lambda}$, in dimensional quantities.

It is possible to split the error $\mathrm{err}(N_{\Delta\tau}, N_M;\mu)$ defined in Eq. (9) in two contributions, as $\mathrm{err}(N_{\Delta\tau}, N_M;\mu) = \varepsilon_{\Delta\tau}(N_{\Delta\tau}, N_M;\mu) + \varepsilon_M(N_{\Delta\tau}, N_M;\mu)$. In Section 2, we introduced the numerical solution (Eq. (7)) and the quasi-analytical solution (Eq. (8)) of interest in the current error analysis. We recall here below the previous definitions:

$$\bar{\phi}_N^{k+1} := \frac{3}{4\pi}\sum_{j=1}^{N_M} x_{j,N}^{k+1}\langle\psi_j|1\rangle \tag{10}$$

constitutes the numerical solution (Eq. (7)), with the temporal coefficients $x_{j,N}^{k+1}$ calculated according to Eq. (6). The quasi-analytic solution (Eq. (8)) is:

$$\bar{\phi}_A^{k+1} := \frac{3}{4\pi}\sum_{j=1}^{CN_M} x_{j,A}^{k+1}\langle\psi_j|1\rangle \tag{11}$$

where the temporal coefficients $x_{j,A}^{k+1}$ come from the quasi-analytic solution of Eq. (5).

It is possible to split the aforementioned error $\mathrm{err}(N_{\Delta\tau}, N_M;\mu)$ (Eq. (9)) by considering that:

$$\bar{\phi}_A^{k+1} - \bar{\phi}_N^{k+1} = \frac{3}{4\pi}\sum_{j=1}^{CN_M} x_{j,A}^{k+1}\langle\psi_j|1\rangle - \frac{3}{4\pi}\sum_{j=1}^{N_M} x_{j,N}^{k+1}\langle\psi_j|1\rangle = \frac{3}{4\pi}\sum_{j=1}^{N_M}\left(x_{j,A}^{k+1}-x_{j,N}^{k+1}\right)\langle\psi_j|1\rangle + \sum_{j=N_M+1}^{CN_M} x_{j,A}^{k+1}\langle\psi_j|1\rangle \tag{12}$$

Then, we define the temporal contribution to the error as

$$\varepsilon_{\Delta\tau}(N_{\Delta\tau}, N_M;\mu) := \frac{\sum_{j=1}^{N_M}\left(x_{j,A}^{k+1}-x_{j,N}^{k+1}\right)\langle\psi_j|1\rangle}{\sum_{j=1}^{CN_M} x_{j,A}^{k+1}\langle\psi_j|1\rangle} \tag{13}$$

and the modal contribution as

$$\varepsilon_M(N_{\Delta\tau}, N_M;\mu) := \frac{\sum_{j=N_M+1}^{CN_M} x_{j,A}^{k+1}\langle\psi_j|1\rangle}{\sum_{j=1}^{CN_M} x_{j,A}^{k+1}\langle\psi_j|1\rangle} \tag{14}$$

Afterwards, we write:

$$|\mathrm{err}(N_{\Delta\tau}, N_M;\mu)| = |\varepsilon_{\Delta\tau}(N_{\Delta\tau}, N_M;\mu) + \varepsilon_M(N_{\Delta\tau}, N_M;\mu) \times| \le |\varepsilon_{\Delta\tau}(N_{\Delta\tau}, N_M;\mu)| + |\varepsilon_M(N_{\Delta\tau}, N_M;\mu)| \tag{15}$$

in which we exploited the triangular inequality to define an upper bound on the error, namely, the right-hand side of the inequality,

Table 1
Values of the adopted parameters in the exemplative error analysis regarding the stable fission products, the long-lived fission product ^{134}Cs and the short-lived fission product ^{131}I.

Nuclide	D (m^2s^{-1})	a (μm)	λ (s^{-1})	μ (/)	t_e (s)	$\tau_e = t_eD/a^2$ (/)
Stable gas	10^{-20}	5	0	0	1.3×10^9	5.1×10^{-1}
^{134}Cs	10^{-20}	5	1.064×10^{-8}	26.6	3.4×10^8	2.2×10^{-2}
^{131}I	10^{-20}	5	9.98×10^{-7}	2495.0	5.0×10^6	2.4×10^{-4}

$|\varepsilon_{\Delta\tau}(N_{\Delta\tau}, N_M;\mu)| + |\varepsilon_M(N_{\Delta\tau}, N_M;\mu)|$.

The temporal contribution to the error $|\varepsilon_{\Delta\tau}(N_{\Delta\tau}, N_M;\mu)|$ (Eq. (13)) is the difference between quasi-analytical and numerical solutions, computed with the same number of modes N_M, hence representing the error due to time discretization. The second contribution to the error, $|\varepsilon_M(N_{\Delta\tau}, N_M;\mu)|$ (Eq. (14)), is the remainder of the modal expansion considered in the numerical solution, truncated at the N_M-term. Thanks to the triangular inequality, the right-hand side of Eq. (15) provides an upper bound on the error introduced by the spectral diffusion algorithm. From now on, we indicate this upper bound as:

$$\varepsilon(N_{\Delta\tau}, N_M;\mu) := |\varepsilon_{\Delta\tau}(N_{\Delta\tau}, N_M;\mu)| + |\varepsilon_M(N_{\Delta\tau}, N_M;\mu)| \quad (16)$$

The upper bound on the error, defined with Eq. (16), varies by changing the spectrum-temporal discretization parameters $(N_{\Delta\tau}, N_M)$ and according to the value of μ. The study of the behaviour of $\varepsilon(N_{\Delta\tau}, N_M;\mu)$ with varying $N_{\Delta\tau}$, N_M and μ configures our next error analyses. Given the definition $\mu = \lambda a^2/D$, we distinguish the $\mu = 0$ case (stable fission products) from the $\mu > 0$ case (radioactive fission products). Indeed:

- Stable fission products are characterized by $\mu = 0$, regardless of a and D. The error map $\varepsilon(N_{\Delta\tau}, N_M;\mu = 0)$ does not depend on a and D, and a single error analysis applies to different reactor conditions.
- Radioactive fission products are characterized by $\mu > 0$. Therefore, depending on its value, we observe different behaviours of $\varepsilon(N_{\Delta\tau}, N_M;\mu)$, according to the considered reactor condition (i.e., the value of μ).

We perform, in Section 3.1, the error analysis in constant conditions ($\mu = \mu_0$) and, in Section 3.2, in time-varying conditions ($\mu = \mu(\tau)$).

3.1. Constant conditions

We showcase illustrative error analyses performed in constant conditions. We consider stable fission products, ^{131}I (short-lived fission product) and ^{134}Cs (long-lived fission product). Respectively, μ takes the values $\mu = 0$, $\mu \approx 26.6$ and $\mu \approx 2495.0$ (numerical values of grain radius a and diffusivity D come from exemplative average values in an LWR pellet and are reported in Table 1).

The error analysis is performed as follows:

1. For a given value of μ, we compute several times the numerical solution (Eq. (7)) with $(N_{\Delta\tau}, N_M)$ that range from (10, 10) up to (1000, 100). The value of μ is kept constant during the interval $(0, \tau_e)$.
2. Similarly, the quasi-analytical solution (Eq. (8)) is computed, with $M = C = 10$.
3. We evaluate the temporal contribution to the error $|\varepsilon_{\Delta\tau}(N_{\Delta\tau}, N_M;\mu)|$ (Eq. (13)), the modal contribution to the error $|\varepsilon_M(N_{\Delta\tau}, N_M;\mu)|$ (Eq. (14)) and the upper bound $\varepsilon(N_{\Delta\tau}, N_M;\mu)$ (Eq. (16)).

We restrict our error analysis up to a mode number $N_M = 100$ and a time-step number $N_{\Delta\tau} = 1000$ to ensure reasonable CPU times and memory use. In Fig. 1, we show $\varepsilon(N_{\Delta\tau}, N_M;\mu)$, $|\varepsilon_{\Delta\tau}(N_{\Delta\tau}, N_M;\mu)|$ and $|\varepsilon_M(N_{\Delta\tau}, N_M;\mu)|$, for the stable (Fig. 1a) and radioactive volatile fission products (Fig. 1b and c) in Table 1.

In the first place, we briefly discuss the main results of error analysis. Namely, the behaviour of the upper bound $\varepsilon(N_{\Delta\tau}, N_M;\mu)$, with respect to the number of time steps $N_{\Delta\tau}$, the number of modes N_M and $\mu = \lambda a^2/D$, the parameter which condenses the information about the described physical phenomenon.

The computed upper bounds $\varepsilon(N_{\Delta\tau}, N_M;\mu)$ are shown on the right side of Fig. 1, for the cases $\mu = 0$ (Fig. 1a), $\mu = 26.6$ (Fig. 1b) and $\mu = 2495.0$ (Fig. 1c). By observing $\varepsilon(N_{\Delta\tau}, N_M;\mu)$ for these three cases, we notice that $\varepsilon(N_{\Delta\tau}, N_M;\mu)$ decreases with increasing $N_{\Delta\tau}$ and N_M, as expected. The major difference regards the rapidity (i.e., the convergence rate) with which the upper bounds $\varepsilon(N_{\Delta\tau}, N_M;\mu)$ decrease by increasing the number of modes N_M in contrast to the reduction of $\varepsilon(N_{\Delta\tau}, N_M;\mu)$ with increasing number of time steps $N_{\Delta\tau}$ (see $|\varepsilon_{\Delta\tau}(N_{\Delta\tau}, N_M;\mu)|$ in Fig. 1a, 1b, c).

The methodology that we provide in Section 4 allows a more precise evaluation of the behaviour of $\varepsilon(N_{\Delta\tau}, N_M;\mu)$, in constant conditions, for a suitable range of values of μ. We limit here the discussion by noting that, for a reasonable number of employed modes ($N_M \approx 20 \div 30$ modes) the major contribution to $\varepsilon(N_{\Delta\tau}, N_M;\mu)$ is represented by the temporal contribution $|\varepsilon_{\Delta\tau}(N_{\Delta\tau}, N_M;\mu)|$, rather than the modal one. This translates in the recommendation that is convenient to increase the number of time steps first, and subsequently the number of modes, to improve the accuracy of the spectral diffusion algorithm.

The behaviour of the contributions $|\varepsilon_{\Delta\tau}(N_{\Delta\tau}, N_M;\mu)|$ and $|\varepsilon_M(N_{\Delta\tau}, N_M;\mu)|$, shown on the left and the middle of Fig. 1, respectively, suffers from numerical artefacts that are noticeable only when these contributes are separately assessed. For this reason, they are not of concern in the present discussion. Nevertheless, we report them for completeness:

- The decrease of $|\varepsilon_{\Delta\tau}(N_{\Delta\tau}, N_M;\mu)||$, at a fixed number of time steps $N_{\Delta\tau} \approx 1000$, by reducing N_M (Fig. 1a and 1b).
- The increase of $|\varepsilon_M(N_{\Delta\tau}, N_M;\mu)||$, at a fixed number of modes $N_{\Delta\tau} \approx 1000$, by increasing N_M (Fig. 1a and 1b, ac).

We indicate the aforementioned trends of $|\varepsilon_{\Delta\tau}(N_{\Delta\tau}, N_M;\mu)||$ and $|\varepsilon_M(N_{\Delta\tau}, N_M;\mu)||$ as artefact because their nature is merely numerical. Indeed, they are ascribable to the definitions given in Eq. (13) and Eq. (14), and in their turn to the behaviour of term $\exp(-\Lambda_n\Delta\tau)$, and its first-order Taylor expansion $\frac{1}{1+\Lambda_n\Delta\tau}$, at large time step size $\Delta\tau$ and small values of μ.

3.2. Random-varying conditions

We show the results of the error analysis performed in time-varying conditions, highlighting the similarities and differences with respect to the case of constant conditions. To account for time-varying conditions, we solve Eq. (2) with a time-dependent $\mu = \mu(\tau)$. In particular, we carry out the analysis exploiting the *random*

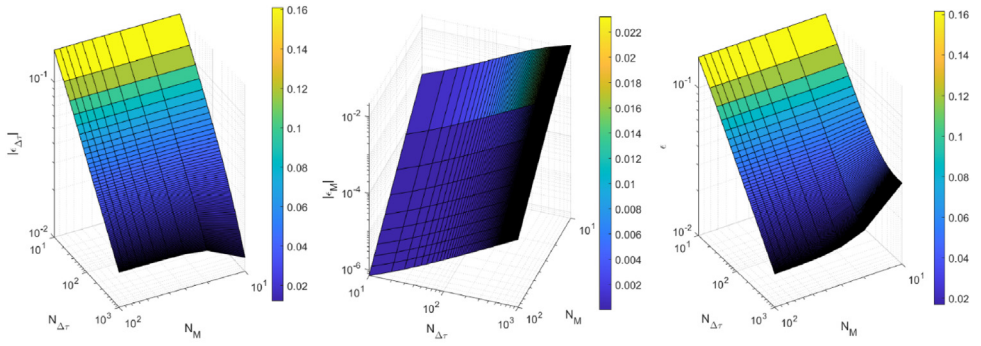

(a) Stable gas ($\mu = 0$)

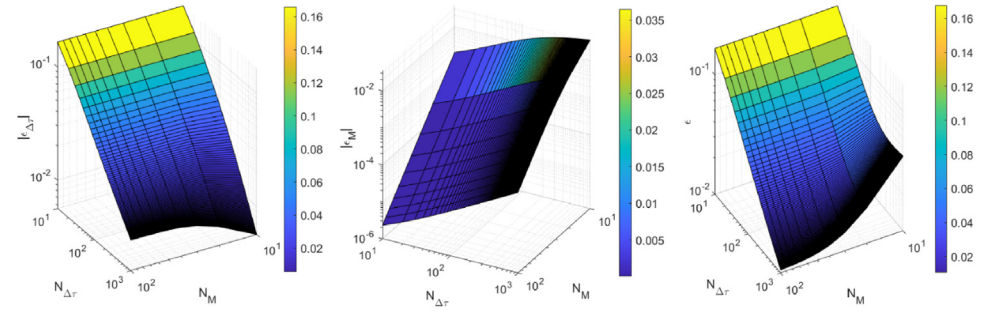

(b) ^{134}Cs ($\mu = 26.6$)

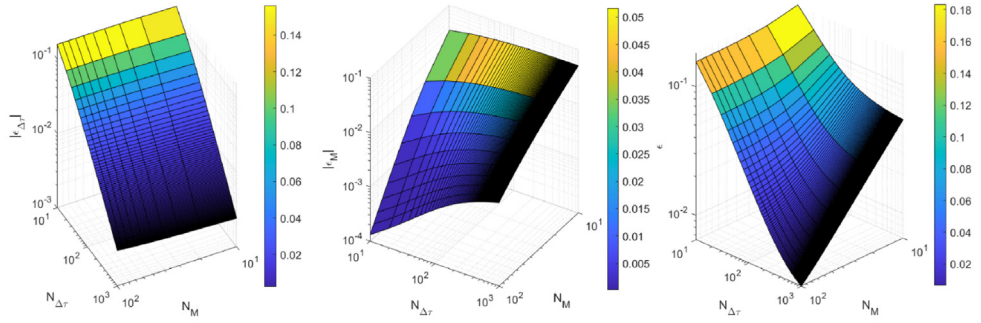

(c) ^{131}I ($\mu = 2495.0$)

Fig. 1. Results of the error analysis in constant conditions. Each horizontal set of figures shows the temporal contribution to the error $|\varepsilon_{\Delta\tau}(N_{\Delta\tau}, N_M; \mu)|$ on the left, the modal contribution to the error $\varepsilon_M(N_{\Delta\tau}, N_M; \mu)$ in the middle, and the upper bound $\varepsilon(N_{\Delta\tau}, N_M; \mu)$ on the right, for a given μ.

or *stochastic-testing* approach [24,25]. Namely, we iterate $N_{\text{iter}} = 100$ times the following procedure:

1. We sample an array for $\mu(\tau)$, with values uniformly distributed between 0 and $\mu_{\max} = 10^9$. The value of $\mu_{\max}$ is arbitrarily set.
2. As previously done (Section 3.1), we compute the numerical solution $\overline{\phi}_N$ (Eq. (7)) and the quasi-analytical solution $\overline{\phi}_A$ (Eq. (8)).[1]
3. We evaluate $|\varepsilon_{\Delta\tau,i}(N_{\Delta\tau}, N_M; \mu)|$ (Eq. (13)), $|\varepsilon_{M,i}(N_{\Delta\tau}, N_M; \mu)|$ (Eq. (14)) and $\varepsilon_i(N_{\Delta\tau}, N_M; \mu)$ (Eq. (16)), where i refers to the i-th iteration.

To obtain an upper bound that is representative for time-varying conditions, we eventually average $|\varepsilon_{\Delta\tau,i}(N_{\Delta\tau}, N_M; \mu)|$, $|\varepsilon_{M,i}(N_{\Delta\tau}, N_M; \mu)|$ and $\varepsilon_i(N_{\Delta\tau}, N_M; \mu)$ over the N_{iter} iterations:

$$\langle|\varepsilon_{\Delta\tau}|\rangle(N_{\Delta\tau}, N_M; \mu) = \frac{1}{N_{\text{iter}}}\sum_{i=1}^{N_{\text{iter}}}|\varepsilon_{\Delta\tau,i}(N_{\Delta\tau}, N_M; \mu)| \tag{17}$$

$$\langle|\varepsilon_M|\rangle(N_{\Delta\tau}, N_M; \mu) = \frac{1}{N_{\text{iter}}}\sum_{i=1}^{N_{\text{iter}}}|\varepsilon_{M,i}(N_{\Delta\tau}, N_M; \mu)| \tag{18}$$

$$\langle\varepsilon\rangle(N_{\Delta\tau}, N_M; \mu) = \frac{1}{N_{\text{iter}}}\sum_{i=1}^{N_{\text{iter}}}\varepsilon_i(N_{\Delta\tau}, N_M; \mu) \tag{19}$$

[1] When assessing time-varying conditions, the numerical solution and quasi-analytical solution are computed on the interval $(0, \tau_e)$, with $\tau_e = \frac{5}{\pi^2+\mu_{\max}/2}$. The value $\mu_{\max}/2$ represents the midpoint of the interval $(0, \mu_{\max})$. The midpoint must be considered because the solution of the diffusion-decay problem (Eq. (2)), in which the decay rate varies between two values (e.g., μ_a and μ_b), can be approximated by the solution of the same diffusion-decay problem with an equivalent, constant, decay rate equal to the midpoint of the interval (μ_a, μ_b). This equivalence is shown below, in Fig. 4.

In Fig. 2 we show the error analysis, performed in time-varying conditions. We compare the latter results with the error analysis performed in constant conditions (as in Section 3.1) with $\mu = 5\times 10^8$, the midpoint of [0,10^9], shown in Fig. 3, to clarify some key differences between constant and time-varying conditions.

We compare the error analysis in time-varying conditions (Fig. 2) with the one in constant conditions (Fig. 3). We recall that the two analyses can be compared each other because of the equivalence between the solution of the diffusion-decay problem (Eq. (2)) in time-varying conditions with the solution of the same problem, in constant conditions, provided that μ is set to the proper midpoint.

Concerning the temporal contributions to the error, $\langle|\varepsilon_{\Delta\tau}|\rangle$ (Fig. 2) and $|\varepsilon_{\Delta\tau}|$ (Fig. 3), we observe an important increase in $\langle|\varepsilon_{\Delta\tau}|\rangle$, due to the steep time variation of μ. Conversely, the modal contributions to the error, $\langle|\varepsilon_M|\rangle$ (Fig. 2) and $|\varepsilon_M|$ (Fig. 3) are unaffected by the time variation of μ. Hence, the increase in the total error ε is only caused by the temporal contribution $\langle|\varepsilon_{\Delta\tau}|\rangle$, and not by the modal one $\langle|\varepsilon_M|\rangle$. We deduce that when we apply the presented spectral diffusion algorithm to a non-stationary diffusion-decay problem, it is highly recommended to increase the number of time steps $N_{\Delta\tau}$ to reduce $\langle|\varepsilon_{\Delta\tau}|\rangle$, and in turn to reduce $\langle\varepsilon\rangle$.

We conclude this section with a visual representation (Fig. 4) of the equivalence exploited before. Namely, that the solution of the diffusion-decay problem (Eq. (2)), in which the decay rate varies between two values (e.g., μ_a and μ_b), can be approximated by the solution of the same diffusion-decay problem with an equivalent, constant, decay rate set to the midpoint of the interval $(\mu_a,\ \mu_b)$.

We compute the numerical solution $\overline{\phi}_N$ (Eq. (7)) of the diffusion-decay problem (Eq. (2)) with a time-varying $\mu(\tau)$. The latter takes values that are randomly sampled from a uniform distribution between 0 and $\mu_{\max} = 10^9$. In particular, we compute $\overline{\phi}_N$ (dashed lines) by going from a "coarse" discretization ($(N_{\Delta\tau},N_M) \sim (10,\ 10)$) to a "fine" one ($(N_{\Delta\tau},N_M) \sim (1000,\ 100)$).

By increasing the discretization parameters, $\overline{\phi}_N$ approaches to the red solid line, that is the numerical solution of the same diffusion-decay problem, with constant $\mu = 5\times 10^8$, the midpoint of [0,10^9]. This confirms that the solution of the diffusion-decay problem (Eq. (2)), in which the μ varies between two values (e.g., μ_a and μ_b), can be satisfactory approximated by the solution of the same diffusion-decay problem with an equivalent, constant, μ equal to the midpoint of the interval $(\mu_a,\ \mu_b)$.

4. Bounding spectrum-temporal discretization parameters

In this section, we provide a simple tool – two reference tables – complementary to the presented spectral diffusion algorithm, to select the spectrum-temporal discretization parameters $(N_{\Delta\tau},N_M)$, providing a suitable upper bound to the numerical error.

To build the tables, we compute a fit of the upper bound $\varepsilon(N_{\Delta\tau},\ N_M;\mu)$, for different values of $\mu = \lambda a^2/D$, namely for different reactor conditions (different values of the diffusion coefficient, different isotopes, etc.).

The fit depends on five parameters, (A, B, C, D, E) and its accuracy is ensured from $R^2 \geq 99.1\%$. The fit function is:

$$\widehat{\varepsilon}\,(N_{\Delta\tau},N_M) = 10^{A\log\,{}_{10}N_{\Delta\tau}\,+\,B} + 10^{C(\,\log_{10}N_M)^2\,+\,D\log\,{}_{10}N_M+E} \tag{20}$$

For each μ, we evaluate $\varepsilon(N_{\Delta\tau},\ N_M;\mu)$ (Eq. (16)), as in Section 3.1, and we obtain A, B, C, D, E for use in Eq. (20). When considering constant conditions, namely when a and D are constant throughout the simulation, we obtain for A, B, C, D and E the values reported in Table 2. Hence, these values allow the computation of the couple $(N_{\Delta\tau},N_M)$ that ensure to get a numerical error lower than $\widehat{\varepsilon}\,(N_{\Delta\tau},N_M)$, when solving the diffusion-decay equation (Eq. (1)) with the presented spectral diffusion algorithm.

It is important to add that, when constant conditions are assessed, we must check if the number of time steps $N_{\Delta\tau}$, given by Table 2, is sufficiently large to bound the numerical error. This is a consequence of having performed the error analysis (Section 3) on the time interval $(0,\tau_e)$, where τ_e is the equilibrium time of the diffusion-decay problem. Indeed, one must check if the time interval of the desired simulation $(0,t_s)$ is larger than the time interval $(0,t_e)$. In other words, if $t_s/t_e \lesseqgtr 1$. Then:

- If $\frac{t_s}{t_e} > 1$, we must correct the number of time steps $N_{\Delta\tau}$ evaluated from Table 2, of a factor t_s/t_e. Therefore, the correction results in the following number of time steps, $\frac{t_s}{t_e}N_{\Delta\tau}$, for use in the simulation, to bound the numerical error.
- If $\frac{t_s}{t_e} < 1$, the number of time steps $N_{\Delta\tau}$ computed from Table 2 is sufficient to bound the numerical error, hence no correction is needed.

This corrective procedure is necessary when assessing diffusion-decay phenomena in constant conditions. Indeed, the error analysis in constant conditions (Section 3) is performed on the interval $(0,\ t_e)$, that is where the transient evolves, i.e., where maximum error is made, when discretizing evolutionary phenomena. Therefore, Table 2 returns the number of time steps $N_{\Delta\tau}$ needed to discretise the diffusion-decay equation on the time interval $(0,t_e)$. In the case $\frac{t_s}{t_e} > 1$, the diffusion-decay phenomenon reaches the equilibrium in a time (t_e) that is lower than the time of the overall time of the simulation (t_s). The consequence is that the transient phase, happening during $(0,\ t_e)$, is discretised with time steps that are larger than the size required $(\Delta t = t_e/N_{\Delta\tau})$ and the upper bound on the numerical error is not guaranteed. The increases in the time step number given by $\frac{t_s}{t_e}N_{\Delta\tau}$ ensure the correct discretization of the entire diffusive phenomenon, and in particular of the transient phase. Lastly, this corrective procedure does not apply to the next

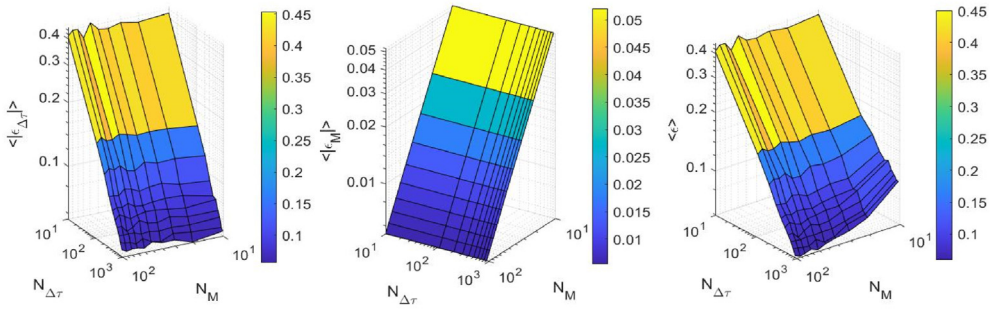

Fig. 2. Error analysis in time-varying conditions, where $\mu(\tau)$takes values in $[0,10^9]$. The average temporal contribution to the error $\langle|\varepsilon_{\Delta\tau}|\rangle$(Eq. (17)) is shown on the left, the average modal contribution to the error $\langle|\varepsilon_M|\rangle$(Eq. (18)) in the middle, and the average total error ε(Eq. (19)) on the right.

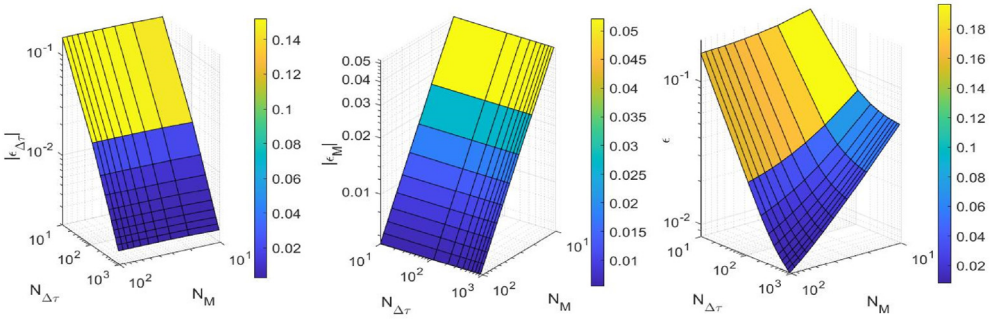

Fig. 3. Error analysis in constant conditions, with $\mu = 5 \times 10^8$, the midpoint of $[0, 10^9]$. The temporal contribution to the error $|\varepsilon_{\Delta\tau}|$ (Eq. (13)) is shown on the left, the modal contribution to the error $|\varepsilon_N|$ (Eq. (14)) in the middle, and the upper bound ε (Eq. (16)) on the right.

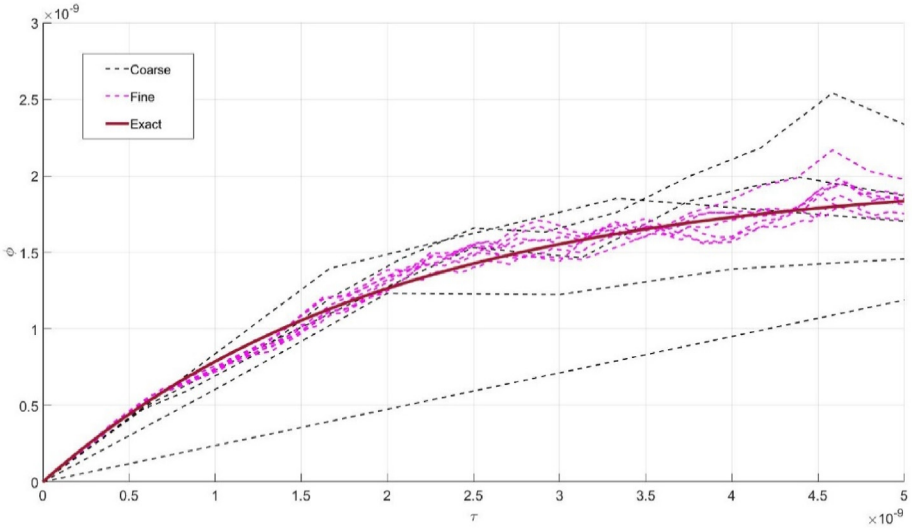

Fig. 4. We show, as dashed lines, the numerical solutions $\overline{\phi}_N$ (Eq. (7)) of the diffusion-decay problem (Eq. (2)), with a time-varying $\mu(\tau)$ that takes values within $[0,10^9]$. Several numerical solutions are shown, according to the adopted discretization, as explained in the text. As red solid line, we show the numerical solution of the same problem, in which a constant $\mu = 5 \times 10^8$ (the midpoint value) is used. As the discretization parameters of the numerical solution increase (that is, going towards the "fine" discretization) the solution in time-varying conditions approaches the one in constant conditions.

Table 3, tailored for time-varying conditions, because in principle we cannot predict where the maximum error happens.

An applicative example of Table 2 is given in Appendix A, where we apply the here below proposed methodology to the simulation of one of the Baker irradiation experiments [26]. We follow these steps:

1. Fix the demanded upper bound (e.g., $U_B = 5\%$).
2. Estimate the constant value of $\mu = \frac{\lambda a^2}{D}$.
3. Determine the row, in Table 2, which best approximate the value previously estimated.

Table 2
Reference table for constant conditions.

μ	A	B	C	D	E
0	−0.5028	−0.2662	−0.0397	−2.8320	1.4450
10	−0.5643	−0.1951	−0.7793	−0.2846	−0.4304
10^2	−0.6998	−0.0498	−0.5863	−0.2571	−0.4280
10^3	−0.8979	0.2502	−0.2448	−0.5961	−0.4140
10^4	−0.9764	0.3470	−0.1205	−0.7202	−0.4080
10^5	−0.9798	0.3367	−0.0841	−0.7575	−0.4062
10^6	−0.9797	0.3343	−0.0731	−0.7687	−0.4057
10^7	−0.9797	0.3340	−0.0702	−0.7716	−0.4056
10^8	−0.9797	0.3340	−0.0698	−0.7720	−0.4055
$>10^8$	−0.9797	0.3340	−0.0698	−0.7720	−0.4055

Table 3
Reference table for time-varying conditions.

$\langle\mu\rangle \in [0, \mu_{max}]$	A	B	C	D	E
[0; 10]	−0.5633	−0.1979	−0.1460	−2.4400	1.3840
[0; 10^2]	−0.4725	−0.1248	−1.1640	1.5660	−1.8260
[0; 10^3]	−0.4705	−0.0781	−0.5503	0.3801	−1.1650
[0; 10^4]	−0.4748	−0.0602	−0.1693	−0.5628	−0.5322
[0; 10^5]	−0.4748	−0.0602	−0.1693	−0.5628	−0.5322
[0; 10^6]	−0.4716	−0.0680	−0.0283	−0.9075	−0.3017
[0; 10^7]	−0.4995	0.0052	−0.0218	−0.9272	−0.2885
[0; 10^8]	−0.4760	−0.0540	−0.0192	−0.9300	−0.2867
[0; 10^9]	−0.4964	−0.0015	−0.0130	−0.9450	−0.3219
[0; 10^{10}]	−0.4912	−0.0143	−0.0130	−0.9450	−0.3219
[0; 10^{20}]	−0.4874	−0.0227	−0.0130	−0.9450	−0.3219
[0; 10^{30}]	−0.4889	−0.0237	−0.0130	−0.9450	−0.3219
[0; 10^{40}]	−0.4716	−0.0581	−0.0130	−0.9450	−0.3219

4. Choose $(N_{\Delta\tau}, N_M)$ for which $\widehat{\varepsilon} \leq U_B$ (if $t_s/t_e > 1$ then use $\frac{N_{\Delta\tau} t_s}{t_e}$) and use it in the implementation of the spectral diffusion algorithm.

We investigate the range $\mu \in [0, 10^9]$ because beyond this upper value we found that the parameters *A, B, C, D, E* become rather insensitive to further increase of μ. Therefore, when diffusion-decay equation is represented by a μ that exceeds 10^9, we recommend referring to the last row of Table 2 (corresponding to $\mu = 10^9$).

Table 3 is designed for application in time-varying conditions. For each row, we operate as in Section 3.2. Namely, when we consider the interval $[0, \mu_{\max}]$, we carry out the error analysis with a value of μ that is randomly sampled within the considered interval. We evaluate ε (Eq. (16)) and we obtain *A, B, C, D, E* for use in Eq. (17).

In time-varying conditions, that is when a and D varying throughout the simulation, the following Table 3 is used to compute the suitable $(N_{\Delta\tau}, N_M)$. An example of the application of this case is given in Appendices B and C, in which we apply the following methodology for the simulation of the VERCORS-4 out-of-pile test and a RIA-representative experiment. The operative procedure to apply Table 3 is the following:

1. Fix the demanded upper bound (e.g., $U_B = 5\%$).
2. Compute the time-varying $\mu = \frac{\lambda a^2}{D}$ and its average value $\langle \mu \rangle$ over the time interval.
3. Determine the row, in Table 3, for which $\mu \in [0, \mu_{max}]$
4. Choose $(N_{\Delta\tau}, N_M)$ for which $\widehat{\varepsilon} \leq U_B$ and use it in the implementation of the spectral diffusion algorithm.

For application in time-varying conditions, we extend the range for μ. Indeed, we reach a maximum value of 10^{40} to take properly into account the variation of μ, strongly affected by the variation of the diffusivity D and temperature T. As before, when the estimated μ exceeds 10^{40}, we recommend referring to the last row of Table 3, corresponding to $\mu \in [0, 10^{40}]$.

Regarding the implementation in a fission gas behaviour module within a fuel performance code, in general such codes entail phenomena of different nature. For example, thermo-mechanical analysis, intra- and inter-granular bubble evolution, etc. If the temporal discretization $N_{\Delta\tau}$is the same for all the involved equations, the proper time-step number $N_{\Delta\tau}$ must be determined to guarantee the accuracy, as well as the convergence, of all the numerical solutions. This means that $N_{\Delta\tau}$is often imposed by other, more binding, requirements. Hence, the mode number N_M is the only parameter which we can set to a reasonable value, according to the radioactive volatile fission products to be modelled, and it can be effectively estimated from Tables 2 and 3. Lastly, the fundamental requirement of the mass conservation must be satisfied inside the fuel grain. For the stable fission gas case, the pure diffusive equation $\left(\frac{\partial C(r,t)}{\partial t} = D(F,T)\nabla^2 C(r,t) + S(F)\right)$ is solved for the average retained concentration together with the production rate equation $\left(\frac{dP(t)}{dt} = S(F)\right)$ and mass conservation results in the evaluation of the fission gas released. Similarly, when the diffusion-decay problem is considered (namely, Eq. (1)) the mass conservation calls for the solution of $\frac{dP(t)}{dt} = S(F) - \lambda P(t)$ (formally identical to Eqs. (5) and (6)) and the balance results again the amount of radioactive fission products released from the grain.

5. Conclusions

This work provides an extensive error analysis of the spectral diffusion algorithm employed in the grain-scale code SCIANTIX. The presented spectral diffusion algorithm allows the accurate modelling the intra-granular behaviour of short-lived volatile fission products through the numerical discretization of the diffusion-decay equation. By defining a suitable upper bound for the numerical error, we carry out an extensive error analysis in a broad range of the spectrum-temporal discretization parameters (number of time steps and modes), during constant and time-varying conditions. The error analysis is of extreme interest in determining the proper number of time steps and modes to be used in implementing the spectral diffusion algorithm in fuel performance codes.

We observe that, especially in time-varying conditions, the contribution to the error due to the temporal discretization is of most concern when determining the numerical error. Conversely, the modal contribution to the error appears to be secondary with respect to the temporal one. This information translates in the recommendation of increase the number of time steps first, and subsequently the number of modes, in order to improve the accuracy of the spectral diffusion algorithm.

We propose a methodology to select the proper *a priori* conditions, in terms of the number of time steps and of modes, to implement the spectral diffusion algorithm and guarantee a correct overestimation of the numerical error. Depending on the simulation (i.e., constant or time-varying conditions), a reference table can be used to accomplish the selection of discretizing parameters. The validity of the methodology is assessed against three cases of practical interest, a Baker's irradiation experiment, a VERCORS-4 experimental test and a RIA-representive experiment.

In conclusion, this work confirms that the presented spectral diffusion algorithm is successfully able to describe diffusive phenomena in transient conditions, by also considering the radioactive behaviour. Since the formulation of the spectral diffusion algorithm is kept simple, the implementation in fission gas behaviour modules of fuel performance codes is straightforward. Moreover, the proposed methodology to bound the numerical error by the *a priori* estimation of the number of time steps and modes, makes the spectral diffusion algorithm more reliable in modelling the intra-granular behaviour of radioactive volatile fission products, in constant and time-varying conditions.

Declaration of competing interest

The authors declare that they have no known competing financial interests or personal relationships that could have appeared to influence the work reported in this paper.

Acknowledgements

This project has received funding from the Euratom research and training programme 2014–2018 under grant agreement No 847656.

Appendix A. Application of the proposed methodology: Baker irradiation experiment

In this section, we implement the spectral diffusion algorithm, presented in Section 2, to model a diffusive problem in stationary conditions and we exploit the methodology outlined in Section 4, in

the proper setting of the spectrum-temporal discretization parameters.

We consider one of Baker's irradiation experiment [27]. These experiments involve UO_2 samples irradiated at a fixed temperature T (we consider the one at $T = 1473$ K) up to a burn-up of 23 GWd/t. We assume a constant fission rate $F = 10^{19}$ fiss m^{-3} s^{-1} and a constant grain radius $a = 5$ μm throughout the 5500 h of irradiation. The diffusivity is $D \approx 1.31 \times 10^{-19}$ m^2 s^{-1}, according to Turnbull formulation [19].

We remember the methodology to apply Table 2:

1. Fix the demanded upper bound (e.g., $U_B = 5\%$).
2. Estimate the constant value of $\mu = \frac{\lambda a^2}{D}$.
3. Determine the row, in Table 2, which best approximate the value previously estimated.
4. Choose $(N_{\Delta\tau}, N_M)$ for which $\widehat{\varepsilon} \leq U_B$ (if $t_s/t_e > 1$ then use $\frac{N_{\Delta\tau} t_s}{t_e}$) and use it in the implementation of the spectral diffusion algorithm.

We demand $U_B = 3$ %, for the maximum error introduced by the spectral diffusion algorithm. Since we deal with stable gas, $\mu = 0$ (see Fig. 5) and, in Table 2, we refer to the first row. By setting $N_{\Delta\tau} = 400$ and $N_M = 40$ the guaranteed bound is $U_B \approx 2.72$ %. There is no need to increase $N_{\Delta\tau}$ because the equilibrium time for the reproduced phenomenon is $t_e \approx 2.7 \times 10^4$ h.

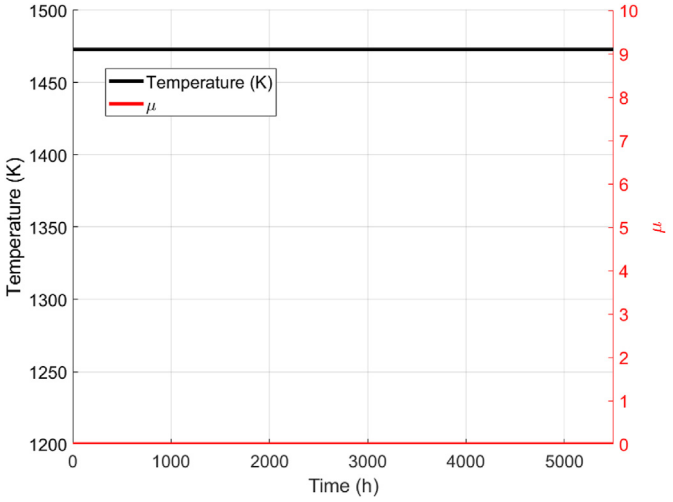

Fig. 5. Constant values for the temperature (black line) and μ (red line) used for the application of Table 2 in constant conditions.

Therefore, by solving the diffusion-decay problem (Eq. (1)) for stable fission gas ($\lambda = 0$) with $N_{\Delta\tau} = 400$ and $N_M = 40$, the error introduced by the spectral diffusion algorithm is below the demanded upper bound ($U_B = 3$ %).

To verify the application of Table 2, we solve the (dimensional) diffusion-decay problem (Eq. (1)) and compute the quasi-analytical and the numerical solution for the concentration $\overline{C}(t)$. The maximum error obtained, according to the definition given by Eq. (9), is err ≈ 1.31 %, below the demanded bound.

Appendix B. Application of the proposed methodology: VERCORS-4

The VERCORS program encompasses six out-of-pile tests on UO_2 samples. It is devoted to the assessment of the release of radioactive fission products from PWR fuel samples, during temperature transients representative of LOCA scenarios [28–30]. In VERCORS-4, three re-irradiated fuel pellets, together with the original cladding, are placed in a furnace. The pellets undergo a temperature transient and on-line fission product release measurements are accomplished [28]. It is important to consider re-irradiated pellets because of the rebuilding of the short-lived fission product inventory, at both intra- and inter-granular level.

We implement the spectral diffusion algorithm presented in Section 2 and we reproduce the intra-granular behaviour of radioactive volatile fission products, according to Eq. (1), during the VERCORS-4 test. To select $(N_{\Delta\tau}, N_M)$ we apply Table 3, by requesting to commit a certain numerical error.

As VERCORS-4 is an annealing test, the fission rate is $F = 0$ fiss m^{-3} s^{-1}, as well as the source term $S(F)$ in the diffusion-decay equation (Eq. (1)). Even if we cannot set $\phi = CD/a^2S$ and comply with the dimensionless analysis developed in Section 2 for $S(F) \neq 0$, the results of the previous dimensionless error analysis, and ultimately the reference tables (Tables 2 and 3), are still valid. In the case of a null source term, together with a finite initial condition $C(r, 0) = C_0$, the diffusion-decay equation is:

$$\frac{\partial C(r,t)}{\partial t} = D(F,T)\nabla^2 C\left(r,t\right) - \lambda C\left(r,t\right),\ r \in [0,a),\ t > 0 \tag{21}$$

The non-dimensional equation is again obtained by posing $\rho = r/a$, $\tau = tD/a^2$, $\phi = CD/a^2C_0$ and $\mu = \lambda a^2/D$. The initial condition is $\phi_0 = D/a^2$. The resulting equation is:

$$\frac{\partial \phi(\rho,\tau)}{\partial \tau} = \tilde{\nabla}^2 \phi(\rho,\tau) - \mu(\tau)\phi(\rho,\tau),\ \rho \in [0,1),\ \tau > 0 \tag{22}$$

Proceeding as in Section 2, we come up with the following formulation for the numerical solution (Eq. (7)):

$$\overline{\phi}_N^{k+1} = \frac{3}{4\pi} \sum_{n=1}^{N_M} \frac{x_{n,N}^k \langle \psi_n | 1 \rangle}{1 + \Lambda_n^{k+1} \Delta\tau} \tag{23}$$

while for the quasi-analytical solution (Eq. (8)) we get:

$$\overline{\phi}_A^{k+1} = \frac{3}{4\pi} \sum_{n=1}^{CN_M} x_{n,A}^k \exp\left(-\Lambda_n^{k+1} \frac{\Delta\tau}{M}\right) \langle \psi_n | 1 \rangle \tag{24}$$

The last two equations, for $\overline{\phi}_N^{k+1}$ and $\overline{\phi}_A^{k+1}$, differ from Eq. (7) and Eq. (8) in the only lack of one term, namely, the one due to the production rate by the source term. In the end, the latter does not affect the results of the error analysis previously developed (Section 3). The definition of the upper bound (Eq. (16)) remain valid and the reference tables (Tables 2 and 3) are still appliable to Eq. (21).

We repeat here the methodology for the application of Table 3:

1. Fix the demanded upper bound (e.g., $U_B = 5\%$).
2. Compute the time-varying $\mu = \frac{\lambda a^2}{D}$ and its average value $\langle \mu \rangle$ over the time interval.
3. Determine the row, in Table 3, for which $\mu \in [0, \mu_{max}]$
4. Choose $(N_{\Delta\tau}, N_M)$ for which $\widehat{\varepsilon} \leq U_B$ and use it in the implementation of the spectral diffusion algorithm.

The determined couple $(N_{\Delta\tau}, N_M)$ therefore ensures that the numerical error introduced by the spectral diffusion algorithm is below the demanded upper bound. As an example, we only consider the radioactive volatile fission product ^{131}I, with decay rate $\lambda = 9.98 \times 10^{-7}$ s^{-1}. We select an upper bound on the error $U_B = 3\%$. Then, we recover the behaviour of the intra-granular diffusivity D from the Turnbull model [19] and the grain radius a behaviour from the Ainscough model [31].

We compute the time-varying $\mu = \lambda a^2/D$ and its average value $\langle \mu \rangle = 1.1 \times 10^{35}$ (Fig. 6). Since the average belongs to the interval $[0, 10^{40}]$, we refer to the last row of Table 3. We choose $N_{\Delta\tau} = 1368$

and $N_M = 40$. From Table 3 we get an upper bound $\hat{\varepsilon} \approx 2.71\,\%$. Namely, by solving the diffusion-decay problem (Eq. (1)) for ^{131}I, with $N_{\Delta\tau} = 1368$ and $N_M = 40$, the error introduced by the spectral diffusion algorithm is below the demanded upper bound ($U_B = 3\%$).

To verify the latter conclusion, we solve the (dimensional) diffusion-decay problem (Eq. (1)) for ^{131}I and compute the quasi-analytical and the numerical solution for the iodine concentration $\overline{C}(t)$. We evaluate the maximum numerical error according to Eq. (9) and we get err $\approx 1.46\,\%$, which is below the demanded error bound, $U_B = 3\%$, as guaranteed by the provided methodology.

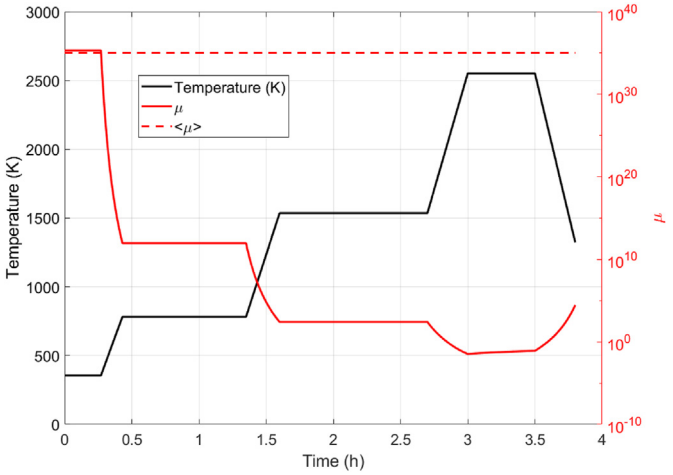

Fig. 6. Temperature transient (solid black line) imposed to UO_2 samples in VERCORS-4 test, used as input in the simulation. The time-varying μ is shown as a red solid line while its average, used in Table 3, is the red dashed line.

Appendix C. Application of the proposed methodology: RIA

As far as the safety analysis is concerned, we consider an experiment that is representative of a Reactivity-Initiated Accident (RIA), a design basis accident for light water reactors [9]. The RIA scenario involves a fast increase of the reactor fission rate, power and temperature during a short period of time, typically tens of millisecond [32,33]. For the application of our error bound methodology, it is an exemplificative case of great interest because the intra-granular concentration of the gaseous and volatile fission products significantly varies in a short amount of time and a robust numerical algorithm is required to follow such evolution. The main scope of this section is hence to verify our methodology against a case in which the temporal evolution develops over a short amount of time, nevertheless we highlight that a complete safety analysis of the nuclear fuel behaviour in RIA conditions is out of the scope.

We consider the CABRI REP-Na5 experiment in which a Gaussian-type power pulse injects 451 J g^{-1} in a rodlet of UO_2/Zr-4 irradiated to 64 GWd t_{HM}^{-1} [31]. Like the previous VERCORS-4 case we use the spectral diffusion algorithm presented in Section 2 to reproduce the intra-granular behaviour of a radioactive volatile fission product. During fast and significant temperature transient several phenomena impact the fission product diffusivity. Since the basis scope of the present analysis is to purely assess the numerical accuracy of our algorithm, we exploit the same models for diffusivity D and grain radius a models [19,30] that we exploited in the previous section (Appendix B).

The expressions for $\overline{\phi}_N^{k+1}$ and $\overline{\phi}_A^{k+1}$ are given by Eq. (7) and Eq. (8). We consider the short-lived gaseous fission product ^{133}Xe, with decay rate $\lambda = 1.53 \times 10^{-6}$ s^{-1}. We evaluate the time-varying $\mu = \lambda a^2/D$ and its average value $\langle\mu\rangle = 4.24$(Fig. 7). From Table 3, we choose $N_{\Delta\tau} = 3010$ and $N_M = 40$ for an upper bound $\hat{\varepsilon} \approx 0.82\%$. In conclusion, by solving the diffusion-decay problem (Eq. (1)) for ^{133}Xe, with $N_{\Delta\tau} = 3010$ and $N_M = 40$, the error introduced by the spectral diffusion algorithm is below 0.82% and the demanded upper bound can be set to $U_B = 1\%$.

To verify the methodology, we solve the (dimensional) diffusion-decay problem (Eq. (1)) for the current isotope of interest and compute the quasi-analytical and the numerical solution for $\overline{C}(t)$. We evaluate the maximum numerical error according to Eq. (9) and we get err $\approx 0.00012\%$, which is well below the demanded error bound, $U_B = 1\%$, as guaranteed by the provided methodology.

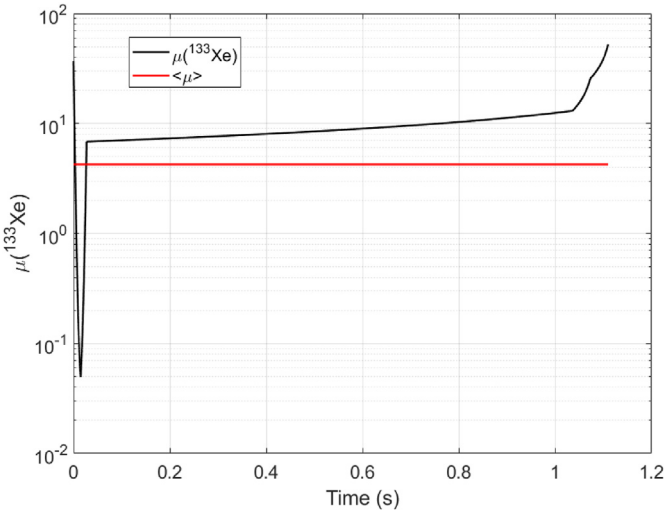

Fig. 7. Time-varying μ(black line) and average value (red line) for the tested transient. The evolution of μmirrors the behaviour of the reproduced RIA case. In particular, the sharp initial variation reflects the strong increase of the production rate typical of this accidental scenario.

Appendix D. Verification against the analytical solution at equilibrium

In stationary condition, the diffusion-decay equation (Eq. (1) or Eq. (2), equivalently) approaches to an equilibrium time-independent value. This is true when $t \geq t_e \approx \frac{5}{\frac{D\pi^2}{a^2}+\lambda}$ or $\tau \geq \tau_e \approx \frac{5}{\pi^2+\mu}$. Since the equilibrium value of the non-dimensional concentration is a function only of μ, we have the opportunity to verify the numerical solution against an exact analytical formula. Given the non-dimensional problem, from the quasi-analytical solution $\overline{\phi}_A$ (Eq. (8)) one can obtain an exact formula for the equilibrium value of $\overline{\phi}$, namely

$$\overline{\phi}_{\mathrm{eq}} = \frac{1}{\mu} - \frac{3}{\mu^{\frac{3}{2}}}\left(\coth\sqrt{\mu} - \frac{1}{\sqrt{\mu}}\right) \tag{25}$$

which only depends on the value of μ. In a similar manner to the previous error analysis, here we show the soundness of the numerical solution $\overline{\phi}_N$ (Eq. (7)) obtained by the presented spectral diffusion algorithm. Since in this section we take as reference solution an exact value both time and mode-independent, our figure of merit is the relative error at exhausted transient

$$\varepsilon(N_{\Delta\tau},\, N_{\mathrm{M}}; \mu) := \frac{\overline{\phi}_{\mathrm{eq}} - \overline{\phi}_N(\tau \geq \tau_e)}{\overline{\phi}_{\mathrm{eq}}} \tag{26}$$

This error depends on the number of time-steps $N_{\Delta\tau}$ and modes N_{M} used in the computation of the numerical solution, and on the value of μ. In Fig. 8 we show the result of an error analysis carried out for $\mu = 26.6$ (a representative case for a ^{131}I isotope, short-lived volatile fission products, in a LWR nuclear fuel in stationary

conditions as reported in Table 1).

The error behaves as expected with respect to $N_{\Delta\tau}$ and N_M, i.e., decreases with their increasing. For sake of brevity, we do not repeat the same analysis for other values of μ since the goal here is to assess the numerical solution against an exact formula for the average concentration (Eq. (25)) and the slight increase of the error with the increase of μ is subjected to the same conclusions drawn in Section 3.1

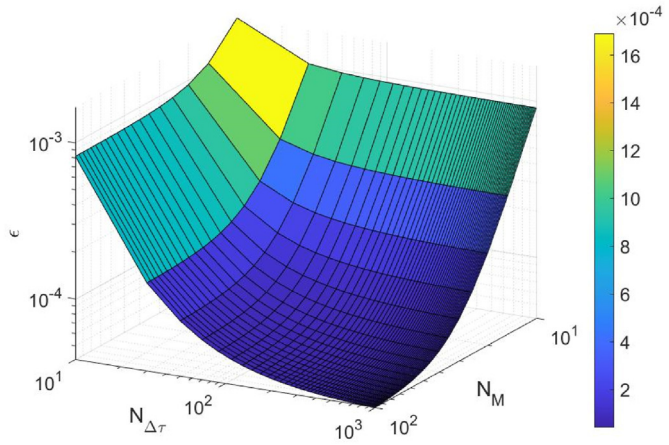

Fig. 8. Behaviour of the relative error on the numerical solution (Eq. (7)) in stationary conditions at exhausted transient, against the analytical equilibrium formula (Eq. (25)). The analysis is performed for $\mu = 26.6$, representative of $a^{131}I$ isotope in typical stationary LWR conditions (see Table 1). By increasing both the number of time-steps and of modes the relative error correctly decreases.

References

[1] J.A. Turnbull, C.E. Beyer, Background and Derivation of ANS-5.4 Standard Fission Product Release Model, *United States Nuclear Regulatory Commision*, 2010, p. 11.

[2] F. D'Auria, C. Camargo, O. Mazzantini, The Best Estimate Plus Uncertainty (BEPU) approach in licensing of current nuclear reactors, Nucl. Eng. Des. 248 (Jul. 2012) 317–328, https://doi.org/10.1016/j.nucengdes.2012.04.002.

[3] L.G. Williams, Overview of international nuclear safety regulation and licensing, in: *Reference Module in Earth Systems and Environmental Sciences*,, Elsevier, 2020, https://doi.org/10.1016/b978-0-12-409548-9.12380-2.

[4] M.S. Veshchunov, V.D. Ozrin, V.E. Shestak, V.I. Tarasov, R. Dubourg, G. Nicaise, Development of the mechanistic code MFPR for modelling fission-product release from irradiated UO_2 fuel, Nucl. Eng. Des. 236 (2) (2006) 179–200, https://doi.org/10.1016/j.nucengdes.2005.08.006.

[5] K. Lassmann, TRANSURANUS: A Fuel Rod Analysis Code Ready for Use, in: Nuclear Materials for Fission Reactors, 1992, pp. 295–302, https://doi.org/10.1016/b978-0-444-89571-4.50046-3.

[6] R.L. Williamson, et al., Validating the BISON fuel performance code to integral LWR experiments, Nucl. Eng. Des. 301 (May 2016) 232–244, https://doi.org/10.1016/j.nucengdes.2016.02.020.

[7] G. Pastore, D. Pizzocri, C. Rabiti, T. Barani, P. van Uffelen, L. Luzzi, An effective numerical algorithm for intra-granular fission gas release during non-equilibrium trapping and resolution, J. Nucl. Mater. 509 (2018) 687–699, https://doi.org/10.1016/j.jnucmat.2018.07.030.

[8] D. Pizzocri, C. Rabiti, L. Luzzi, T. Barani, P. Van Uffelen, G. Pastore, PolyPole-1: an accurate numerical algorithm for intra-granular fission gas release, J. Nucl. Mater. 478 (2016) 333–342, https://doi.org/10.1016/j.jnucmat.2016.06.028.

[9] V. Georgenthum, et al., SCANAIR-BISON Benchmark on CIP0-1 RIA Test, 2017.

[10] D. Pizzocri, T. Barani, L. Luzzi, SCIANTIX: a new open source multi-scale code for fission gas behaviour modelling designed for nuclear fuel performance codes, J. Nucl. Mater. 532 (2020) 152042, https://doi.org/10.1016/j.jnucmat.2020.152042.

[11] P. Hermansson, A.R. Massih, An effective method for calculation of diffusive flow in spherical grains, J. Nucl. Mater. 304 (2–3) (2002) 204–211, https://doi.org/10.1016/S0022-3115(02)00873-5.

[12] K. Forsberg, A.R. Massih, Fission gas release under time-varying conditions, J. Nucl. Mater. 127 (2–3) (1985), https://doi.org/10.1016/0022-3115(85)90348-4.

[13] K. Forsberg, A.R. Massih, Diffusion theory of fission gas migration in irradiated nuclear fuel UO_2, J. Nucl. Mater. 135 (2–3) (1985), https://doi.org/10.1016/0022-3115(85)90071-6.

[14] A.H. Booth, A Method of Calculating Fission Gas Diffusion from UO_2 Fuel and its Application to the X-2-F Loop Test, *Atomic Energy of Canada Limited*, 1957.

[15] D.R. Olander, Fundamental Aspects of Nuclear Reactor Fuel Elements, Technical Information Center Energy Research and Development Administration, 1976.

[16] R.J. White, M.O. Tucker, A new fission-gas release model, J. Nucl. Mater. 118 (1) (1983) 1–38, https://doi.org/10.1016/0022-3115(83)90176-9.

[17] P. Van Uffelen, R.J.M. Konings, C. Vitanza, J. Tulenko, Analysis of Reactor Fuel Rod Behavior, in: D.G. Cacuci (Ed.), Handbook of Nuclear Engineering, first ed., Springer, US, 2010.

[18] J. Rest, M.W.D. Cooper, J. Spino, J.A. Turnbull, P. Van Uffelen, C.T. Walker, Fission gas release from UO_2 nuclear fuel: a review, J. Nucl. Mater. 513 (2019) 310–345, https://doi.org/10.1016/j.jnucmat.2018.08.019.

[19] J.A. Turnbull, C.A. Friskney, J.R. Findlay, F.A. Johnson, A.J. Walter, The diffusion coefficients of gaseous and volatile species during the irradiation of uranium dioxide, J. Nucl. Mater. 107 (2–3) (1982) 168–184, https://doi.org/10.1016/0022-3115(82)90419-6.

[20] K. Lassmann, H. Benk, Numerical algorithms for intragranular fission gas release, J. Nucl. Mater. 280 (2) (2000) 127–135, https://doi.org/10.1016/S0022-3115(00)00044-1.

[21] W.N. Rausch, F.E. Panisko, ANS54: a Computer Subroutine for Predicting Fission Gas Release, Pacific Northwest Laboratory, USA, 1979.

[22] S. Sengupta, T.K. Sengupta, J.K. Puttam, K.S. Vajjala, Global spectral analysis for convection-diffusion-reaction equation in one and two-dimensions: effects of numerical anti-diffusion and dispersion, J. Comput. Phys. 408 (2020) 109310, https://doi.org/10.1016/j.jcp.2020.109310.

[23] V.K. Suman, T.K. Sengupta, C. Jyothi Durga Prasad, K. Surya Mohan, D. Sanwalia, Spectral analysis of finite difference schemes for convection diffusion equation, Comput. Fluid 150 (2017) 95–114, https://doi.org/10.1016/j.compfluid.2017.04.009.

[24] T.K. Sengupta, A. Dipankar, P. Sagaut, Error dynamics: beyond von Neumann analysis, J. Comput. Phys. 226 (2) (2007) 1211–1218, https://doi.org/10.1016/j.jcp.2007.06.001.

[25] R. Hamlet, "Random Testing," in *Encyclopedia of Software Engineering*, John Wiley & Sons, Inc., Hoboken, NJ, USA, 2002, https://doi.org/10.1002/0471028959.sof268.

[26] P. Tramontana, D. Amalfitano, N. Amatucci, A. Memon, A.R. Fasolino, Developing and evaluating objective termination criteria for random testing, ACM Trans. Software Eng. Methodol. 28 (3) (Jun. 2019), https://doi.org/10.1145/3339836.

[27] C. Baker, The fission gas bubbles distribution in uranium dioxide from high temperature irradiated SGHWR fuel pins, J. Nucl. Mater. 66 (1977) 283–291.

[28] G. Ducros, P.P. Malgouyres, M. Kissane, D. Boulaud, M. Durin, Fission product release under severe accidental conditions: general presentation of the program and synthesis of VERCORS 1-6 results, Nucl. Eng. Des. 208 (2) (2001) 191–203, https://doi.org/10.1016/S0029-5493(01)00376-4.

[29] G. Ducros, Y. Pontillon, P.P. Malgouyres, Synthesis of the VERCORS experimental programme: separate-effect experiments on Fission Product release, in support of the PHEBUS-FP programme, Ann. Nucl. Energy 61 (2013) 75–87, https://doi.org/10.1016/j.anucene.2013.02.033.

[30] Y. Pontillon, G. Ducros, Behaviour of fission products under severe PWR accident conditions: the VERCORS experimental programme - Part 2: release and transport of fission gases and volatile fission products, Nucl. Eng. Des. 240 (7) (2010) 1853–1866, https://doi.org/10.1016/j.nucengdes.2009.06.024.

[31] J.B. Ainscough, B.W. Oldfield, J.O. Ware, Isothermal grain growth kinetics in sintered UO_2 pellets, J. Nucl. Mater. 49 (2) (1973) 117–128, https://doi.org/10.1016/0022-3115(73)90001-9.

[32] NEA/CSNI/R(2010)1, Nuclear Fuel Behaviour under Reactivity-Initiated Accident (RIA) Conditions, 2010.

[33] M. Ishikawa, S. Shiozawa, A study of fuel behavior under reactivity initiated accident conditions — review, J. Nucl. Mater. 95 (1–2) (1980) 1–30.